Article

Mapping threatened canga ecosystems in the Brazilian savanna using U-Net deep learning segmentation and Sentinel-2 images: a first step toward conservation planning

Eric Oliveira Pereira[1] iD*, Fabien H. Wagner[2]* iD*, Luciana Hiromi Yoshino Kamino[1]** iD

& Flávio Fonseca do Carmo[1] iD

[1]Instituto Prístino, Rua Três de Maio, 56, Belo Horizonte, MG, Brasil.
[2]University of California, Institute of Environment and Sustainability, Los Angeles, CA, USA.
*Corresponding author:luciana@institutopristino.org.br

Abstract: Canga ecosystems are iron-rich habitats and pose a challenge for conservation and environmental governance in Brazil. They support high levels of biodiversity and endemism and, at the same time, have suffered intense losses and degradation due to large-scale iron ore mining. The Peixe Bravo River Valley in the Brazilian savanna is one of the last natural canga areas that has yet to face the irreversible impacts of mining. However, there are vast gaps in data on the vegetation cover, location, spatial distribution, and area of occurrence of this ecosystem. Therefore, more information is needed on the appropriate scale, without which it is difficult to establish conservation planning and strategies to prevent, mitigate or compensate for impacts on canga ecosystems. In this study, we provide the first map of canga ecosystems in Brazil using the U-Net deep learning model and Sentinel-2 images. In addition, we estimate the degree of direct threat faced by ecosystems due to the spatial overlap of the mapped cangas and the location of mining concession areas for iron ore exploitation. The deep learning algorithm identified and segmented 762 canga patches (overall accuracy of 98.5%) in an area of 30,000 ha in the Peixe Bravo River Valley, demonstrating the high predictive power of the mapping approach. We conclude that the direct threat to canga ecosystems is high since 99.6% of the observed canga patches are included in mining concession areas. We also highlight that the knowledge acquired about the distribution of cangas through the application of an effective method of artificial intelligence and the use of open-source satellite images is especially important for supporting conservation strategies and environmental public policies.

Keywords: Conservation policies; ecosystem monitoring; ironstone; remote sensing; artificial intelligence.

Mapeamento de ecossistemas de canga ameaçados no Cerrado brasileiro utilizando deep learning segmentação U-Net e imagens Sentinel-2: um primeiro passo para o planejamento de conservação

Resumo: Os ecossistemas de Canga, habitats com elevadas concentrações de ferro, são um desafio para conservação e governança ambiental no Brasil. Eles sustentam uma alta biodiversidade e endemismo, e sofreram intensas perdas e degradações de áreas naturais devido à mineração de ferro em larga escala. O Vale do Rio Peixe Bravo, localizado no Cerrado brasileiro, é uma das últimas regiões com ecossistemas de canga que ainda não sofreu impactos irreversíveis da mineração. Mas ainda há ausência de dados sobre a cobertura vegetal, localização, distribuição geográfica e a área de ocorrência desse ecossistema. Portanto, a ausência de informações em escala adequada dificulta o planejamento em conservação e as estratégias para prevenir, mitigar ou compensar os impactos nos ecossistemas de canga. Neste estudo, nós fornecemos o primeiro mapa de ecossistemas de canga no Brasil elaborado a partir de deep learning segmentação U-Net e imagens de satélite Sentinel-2. Além disso, nós estimamos o grau de ameaça direta dos ecossistemas devido a sobreposição espacial das manchas de cangas preditas e a localização dos títulos de concessão minerária para exploração do minério de ferro. O algoritmo de aprendizado profundo identificou 762 manchas de canga (acurácia acima de 98,5%) em uma área de 30.000 ha no Vale do Rio Peixe Bravo, demonstrando o alto poder preditivo do método de mapeamento. Nós estimamos que há um alto grau de ameaça direta aos ecossistemas de canga, uma vez que 99,6% das manchas de cangas preditas estão incluídas em áreas de concessão de mineração. Nós

também destacamos que o conhecimento adquirido sobre a distribuição das cangas por meio da aplicação de um método eficaz de inteligência artificial e do uso de imagens de satélite de código aberto é especialmente importante para apoiar estratégias de conservação e políticas públicas ambientais.

Palavras-chave: *Políticas de conservação; monitoramento de ecossistemas; campos rupestres ferruginosos; sensoriamento remoto; inteligência artificial.*

Introduction

The collapse of natural ecosystems due to human activities is a global crisis, with consequences such as decreased biodiversity, species extinction, environmental degradation, resource depletion, pollution, wealth and climate impacts, poverty, and inequality (Cardinale et al. 2012, UNEP 2019). Large-scale mining is an activity that modifies entire landscapes by removing and processing billions of tons of rocky material every year, causing intense and prolonged socioenvironmental impacts (Carmo et al. 2020). Therefore, the ironstone ecosystems stand out as the natural areas most threatened by mining activities. These iron-rich habitats, known as cangas, are found mainly in restricted areas of Brazil and Australia and support high levels of biological diversity – *sensu* Convention on Biological Diversity (MMA 2000) – and many rare and endemic species (Jacobi et al. 2011, English & Keith 2015, Carmo et al. 2018). The main characteristics of canga ecosystems are their anomalous metal contents (especially natural iron and manganese) and insular distributions, which are island-like lateritic duricrusts that are home to specialized edaphic plant communities (Jacobi et al. 2011, Tibbet 2015). Harsh environmental conditions, in addition to the geographic isolation and the antiquity of the cangas duricrusts, likely contributed to the formation of the evolutionary scenarios responsible for the high number of endemic species, the distributions of which are restricted to one or a few localities (Gibson et al. 2010, Carmo & Kamino 2017, Leme et al. 2020).

The global demand for Brazilian iron ore led to the production of this resource increasing to 510 million tons in 2019 (ANM 2020), with extractions occurring in canga ecosystems. Consequently, mining has caused the loss and degradation of iron-rich habitats, with critical outcomes such as the local extinction of rare plant populations and irreversible damage to surface and underground freshwater reserves (Carmo et al. 2018, Salles et al. 2019). In addition, the destruction of canga ecosystems as a result of large-scale mining causes landscape and aesthetic degradation and environmental conflicts with traditional communities (Sánchez et al. 2018, EJatlas 2021a, b). Most regions with canga ecosystems in Brazil have already experienced the intense loss and degradation of natural areas due to dozens of large-scale mining sites, such as those located in the Serra dos Carajás (Amazon Forest), Morraria do Urucum (Pantanal), Caetité (Caatinga), the Serra da Serpentina and the Quadrilátero Ferrífero (Atlantic Forest). The Quadrilátero Ferrífero has already lost up to 50% of its natural canga ecosystem area (Salles et al. 2019), and most canga remnants are found in a very degraded matrix composed of large-scale open pit mines (Jacobi et al. 2011, Sonter et al. 2014).

One of the last natural areas that has not yet irreversible impacts from mining is in the Peixe Bravo River Valley region (Cerrado, Brazilian savanna), southeastern Brazil (Carmo & Kamino 2017). However, in this region, there is still an unexploited iron ore megadeposit, identified as the Nova Aurora Iron District. Currently, there are several large-scale mining projects in the area (Melfi et al. 2016), and the exploitation of these iron-rich deposits is the main direct threat (sensu Salafsky

et al. 2008) to canga ecosystems. There are limited data available about the vegetation cover, location, distribution, and area of occurrence of the canga ecosystems in the Peixe Bravo River Valley. This lack of information is due to the challenges of accessing remote regions and the high cost of surveys of geological field camps. These limitations of the data are also related to the scale of existing maps, which is usually smaller than 1:100,000, with some maps on the 1:1,000,000 scale. The smallest linear units that can be mapped on these scales are approximately 150 and 3000 meters, respectively, which is not suitable for identifying most canga outcrops (for details see CODEMIG 2012, Souza et al. 2020, CPRM 2021). The lack of information on the appropriate scale precludes conservation planning and the implementation of measures for the prevention and mitigation of impacts or compensation for damage to biodiversity (Hardner et al. 2015). Therefore, the Peixe Bravo River Valley region represents a unique opportunity to develop solution-based conservation research (Fonseca et al. 2021) that can contribute to the reduction in conflicts between local communities, the mining industry, and environmental policies.

The use of remote sensing and artificial intelligence technologies has great potential for supporting conservation planning, including the indication of critical habitats, ecosystem risk assessments and landscape analysis for large-scale monitoring (Christin et al. 2019, Lamba et al. 2019). In the last decade, a revolution for image classification occurred in 2012 using deep learning techniques that began with AlexNet, a convolutional neural network architecture (Krizhevsky et al. 2017). The field of remote sensing has been using deep learning since 2012 to improve its capacity to automatically classify features in satellite images. Using only raw data, supervised deep convolutional networks automatically learn objects in an image with minimal knowledge about those features (LeCun et al. 1998, 2015). For example, for semantic segmentation, the only necessary input is a mask with labels to aid recognition of the training images (Wagner et al. 2019).

The aims of this study were as follows: 1) to identify and map canga ecosystems using Sentinel-2 images and the artificial intelligence tool U-Net convolutional network; 2) after mapping, to estimate the degree of direct threat faced by ecosystems due to the spatial overlap of cangas and the location of mining concession regimes for iron ore exploitation. We also highlight how the knowledge acquired about the distribution of cangas through the application of the U-Net network and the use of open-source satellite images is especially important to support conservation strategies and environmental public policies.

Materials and Methods

1. Study area

The study was conducted in a landscape comprised predominantly of the Cerrado biome (Brazilian savannas) located in the north of the state of Minas Gerais, Brazil, centered at 16°7' S and 42°42' W (Figure 1). The
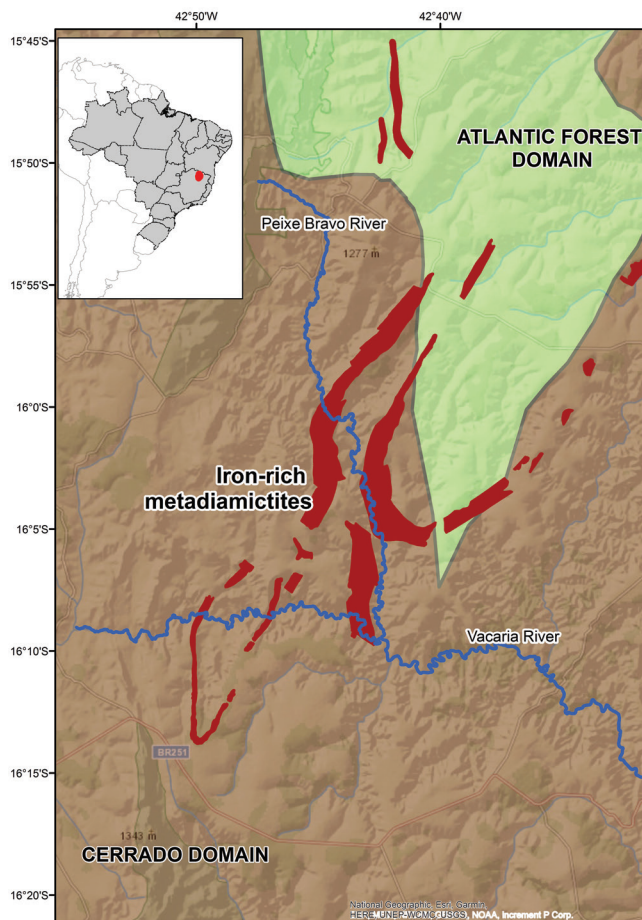
Figure 1. Peixe Bravo River Valley region, North Minas Gerais state, southeastern Brazil. Location of iron-rich metadiamictites from the Riacho Poções Member, in red (Macaúbas Group, Nova Aurora Formation), in the study area. Inset map: South America.

climate in the region is tropical, with a dry winter (Aw type according to Köppen) and an average annual rainfall of approximately 900 mm (Reboita et al. 2015). The canga duricrust is the result of millions of years of weathering of the Neoproterozoic rocks that mainly consist of iron-rich metadiamictites of the Riacho Poções Member (Macaúbas Group, Nova Aurora Formation) (CODEMGE 2018). Extensive plateaus and some hills are the main forms of relief perceived in the landscape. The high topographic heterogeneity of the canga duricrusts forms a set of habitats, such as cracks, depressions, pores, cliffs, puddles and caves, and a corresponding vegetation mosaic (Figure 2).

According to the Technical Manual of Brazilian Vegetation (IBGE 2012), the plant communities associated with canga duricrusts can be defined as relict communities or vegetational refuges, which are adapted to very specific deterministic factors, such as oligotrophic and metalliferous rocky substrates (Carmo & Kamino 2017). Vegetation refuges, therefore, exhibit high sensitivity to any type of intervention since endemic species are abundant. The most frequent phytophysiognomies in canga ecosystems are rocky grasslands and shrublands, known as Campos Rupestres Ferruginosos (Figure 3). This open vegetation occurs in very acidic and oligotrophic metalliferous canga outcrops. Woodland physiognomies can also occur along the canga border and in duricrust cracks and depressions, depending on the topography, soil thickness and moisture (Carmo et al. 2011, Carmo & Kamino 2017).

2. Classification and mapping of the canga ecosystems

2.1. Sentinel-2 images and preprocessing

Since 2015, Sentinel-2 is an orbital mission that has been providing continuous global multispectral images with a spatial resolution of 10 meters, thus, can contribute to the mapping of cangas. Furthermore, Sentinel-2 has a revisit rate of up to five days at the equator (ESA 2015),
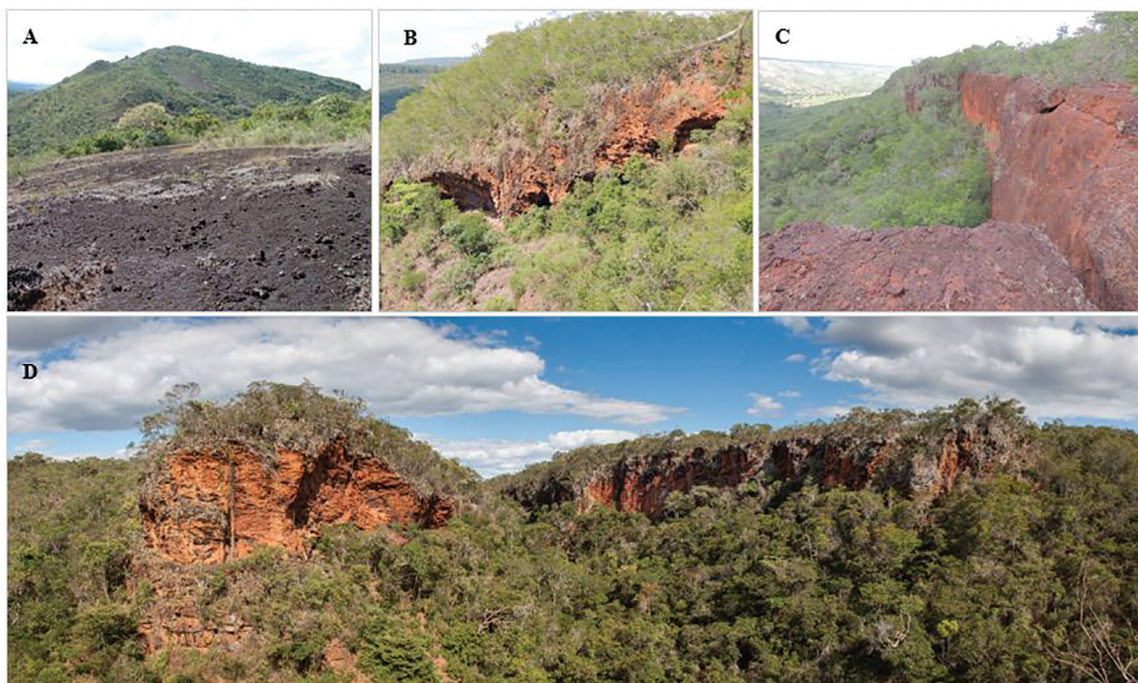

Figure 2. Peixe Bravo River Valley landscape diversity. (A) Hills, (B) caves, (C) cracks and cliffs, and (D) woodland in valleys. Photos: Instituto Prístino.

Figure 3. Canga ecosystems in the Peixe Bravo River Valley, North Minas Gerais state, Brazil. (A) Contrast between the plant communities in iron duricrusts (canga) and the tree matrix outside the canga. (B) Specialized edaphic plant communities in the canga (ironstone) in the foreground and savanna landscape in the background. Photos: Instituto Prístino.

Table 1. Sentinel-2A and Sentinel-2B images used to generate and apply the prediction model for different data corresponding to the passage of the satellite.

Image ID	Original name from Sentinel hub	Date
	Model	
Image 01	S2A_MSIL1C_20190608T130251_N0207_R095_T23LQC_20190608T143715.tif	06/08/2019
Image 03	S2B_MSIL1C_20190703T130259_N0207_R095_T23LQC_20190703T161417.tif	07/03/2019
Image 06	S2A_MSIL1C_20160822T130252_N0204_R095_T23LQC_20160822T130418.tif	08/22/2016
	Prediction	
Image 07	S2A_MSIL1C_20161021T130242_N0204_R095_T23LQC_20161021T130242.tif	10/21/2016
Image 10	S2A_MSIL1C_20170419T130251_N0204_R095_T23LQC_20170419T130247.tif	04/19/2017
Image 11	S2A_MSIL1C_20180124T130241_N0206_R095_T23LQC_20180124T143902.tif	01/24/2018
Image 12	S2A_MSIL1C_20180504T130251_N0206_R095_T23LQC_20180626T123252.tif	06/26/2018
Image 13	S2A_MSIL1C_20190119T130241_N0207_R095_T23LQC_20190119T143228.tif	01/19/2019
Image 14	S2A_MSIL1C_20160713T130431_N0204_R095_T23LQC_20160713T202929.tif	07/13/2016

which can help to determine the best time to map the cangas. For the training of the model, we used three images of the T23LQC tile from the dry period of this region, which occurs between May and September. As shown in Table 1, these images were sensed on 06/08/2019 and 08/22/2016 from Sentinel-2A (prefix S2A) and 07/03/2019 from Sentinel-2B (prefix S2B). For the model predictions, we selected six from different years and periods, including the rainy season sensed in October (Image 07) and January (images 11 and 13) and others sensed in the dry season in May (Image 10), June (Image 12), and July (Image 14). They were all used to identify the potential of the technique for mapping and monitoring. It is important to note that our prediction was applied for each of the images separately, and the training was constructed using the three cited images together.

The occurrence of cangas was mapped from an initial area of 1250 km^2 (50 km × 25 km), obtained from the delimitation of the lithological iron formations available in mappings of the region (scales from 1:100,000 to 1:1,000,000); details are available in the Minas Gerais Mineral Resources web map (CODEMGE 2018). We used Level 1C, Sentinel-2A and 2B images from the European Space Agency (ESA) (Table 1). The Level 1C product resulted from using a digital elevation model to project the image in coordinates. Radiometric measurements per pixel were held on top of atmosphere reflectances with all parameters aimed at transforming them into radiances. In addition, the Level-1C images were resampled with a constant ground sampling distance of 10, 20 and 60 meters depending on the native resolution of the different

spectral bands (ESA 2015). The data were downloaded from the Sentinel Data Hub (2020). The images were organized into tiles that cover 108 × 108 kilometers with 1080 × 1080 pixels. We only used red (665 nm), green (560 nm), blue (490 nm), and infrared (842 nm) spectra, all of them at a spatial resolution of 10 meters. The images were preprocessed so that they could be used for the intended method; preprocessing required rescaling of the digital numbers (DN) from 11 bits to 8 bits. In addition, the bands were unified in a composite band process, borders were inserted around the image, and a cut was made at the limits of the study area. The preprocessing procedures of the scenes were performed in RStudio software (R Core Team 2016). The reference image for the vectorization was Image 01 (Table 1). In addition, Google Earth Pro software (Google 2021) was used to assist with the orientation and verification of canga areas in very high-resolution images.

2.2. U-Net convolutional network

In this study, we used a convolutional network for multiclass image segmentation known as U-nets, with which pixel-by-pixel classification is performed and the probability of each pixel belonging to a particular class is estimated. Details of this architecture can be found in Ronneberger et al. (2015) and Wagner et al. (2019). We adapted the filters to improve performance to reach our aim of classifying a large natural surface and because the sentinel images have a smaller spatial resolution when compared with Ronnerberger et al. (2015) and Wagner et al. (2019). The algorithm for generating the model uses three images from the same region (Table 1). The tests were performed with the composition in the natural color (red, green, blue), as in other works in this field (Wagner et al. 2019, 2020a), and the false-color composition was also tested (infrared, red, green) because of the difference between our target area and regions assessed in other studies. The scripts and data necessary to reproduce the model are available on Zenodo (https://doi.org/10.5281/zenodo.6762185).

To enable the U-Net algorithm to recognize and segment the canga cover, we used a vectorized mask based on an image to indicate the ground truth sample, acquired on 06/08/2019, for training (Table 1). This image was chosen due to the low cloud cover and the greater contrast between the canga vegetation and surrounding vegetation; the incidence of water stress reduced the vegetation cover in the canga ecosystem, while the Brazilian savanna matrix remained unchanged. In addition to vector samples, field data collected in 2015, 2019 and 2020 were used to guide searches and check areas for the occurrence of canga (Figure 4). The field data were obtained using a GPS receiver (Garmin GPS 62S model) with at most ±5 m error and were recorded by a Nikon Coolpix P510 camera and DJI Mavic 2 unmanned aerial vehicle (UAV). We applied the geoprocessing and satellite image interpretation techniques available on 09/23/2003, 08/06/2010, 03/06/2013, 04/23/2014, and 09/12/2019 from Google Earth Pro 7.3.6.9326 (Google LLC. 2022) to extract the polygon (vectorized mask) of the canga areas identified in the field.

Using a script developed in RStudio software (R Core Team 2016), the vector mask was superimposed on Sentinel images 01, 02 and 03 (Table 1). The images were subdivided into 32 × 32 pixel squares. Thus, the value representing canga presence (DN = 1) was assigned only in places where there was overlap between the sample vectors and the images. With the resulting squares, a random draw was made in the remainder of the scene to generate squares with the other types of coverage, which were named background (DN = 0). Thus, squares (tiles) of the object of interest (canga) and their surroundings (background)

were obtained, generating two classes for the model. Ultimately, the sample was composed of 927 images containing canga only or canga plus background and 1,134 images containing background only. Eighty percent (1,649) were used for the training, and 20% (412) were used for the independent validation of the U-Net segmentation.

In addition, during the training process, image processing techniques were applied to the input images to artificially increase the number of images in the training sample and to help the model generalize to improve prediction on new images. This data augmentation was applied randomly to the input images of the model, as follows: rotations of 0/90/180/270 degrees, since its direction affects how the algorithm interprets an object; changes in the brightness, saturation and hue; conversion of the RGB to BSH (brightness-saturation-hue); and modulation of the values between 95% and 110% for brightness, between 95% and 105% for saturation and between 95% and 105% for hue. This was done to reduce overfitting (Kim 2020). More details on this process can be found in Wagner et al. (2019).

The training of the model included stages such as analyzing a first result and making subsequent adjustments based on visual verification of the predictions so that the squares containing false-positive data could be identified. Thus, the squares that were visually identified were added to the randomly drawn background (DN = 0). In the subsequent tests of the constructed model, this adjustment was refined until the best result, which was related to the reduction in false positives in this case, was obtained.
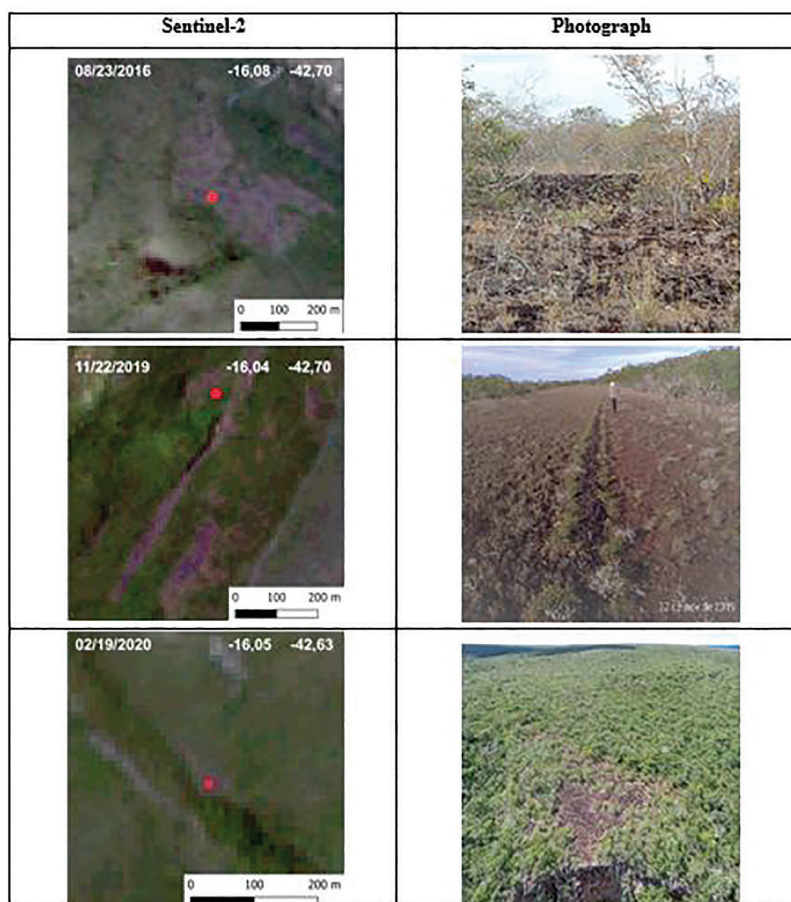

Figure 4. Examples of canga ecosystems observed in Sentinel-2 images and during fieldwork conducted in 2016, 2019 and 2020. Photos: Instituto Prístino.

We randomly sampled images and their associated mask and used 80 percent for training and 20 percent for validation of our classification. Two metrics were estimated for the segmentation accuracy assessment. The first calculates the overall accuracy in terms of percent of well classified pixels (0 or 1), which is implemented by pixelwise assessment. The confusion matrix between the predicted results and the validation sample was generated. The confusion matrix is a table with two rows and two columns that reports the number of canga areas predicted by the U-Net algorithm (correctly predicted), canga predicted where there are no canga (incorrect predicted canga), no canga predicted as no canga (background correctly classified), and no canga predicted as canga (background incorrectly classified). The second metric, the *F*1 score, compares correctly and incorrectly classified segments. The *F*1 score is computed for each class *i* as the harmonic average of the precision and recall (Equation 1), where precision is the ratio of the number of segments correctly classified as *i* and the number of all segments (true and false-positive), and recall is the ratio of the number of segments classified correctly as *i* and the total number of segments belonging to class *i* (true positive and false negative). This score varies between 0 (lowest value) and 1 (best value).

$$F1_i = 2 \; * \; \frac{precision_i * recall_i}{(precision_i + recall_i)}$$

Equation 1: *F*1-Score, where *i* is the number of segments.

To evaluate the prediction and performance of the algorithm, each satellite image (Table 1) was cropped on a regular grid of 320 × 320 pixels, and 64 neighboring pixels were added on each side to create an overlap between the patches. The predictions were made for these images with 384 × 384 pixels, and the resulting images were cropped to 320 × 320 pixels and merged to reconstitute an image of the canga cover to the original extent. This overlapping method was used to prevent prediction artifacts on the image borders, a known problem for the U-Net algorithm (Ronneberger et al. 2015). Classification was made if a pixel prediction value was greater than or equal to 0.5 for a given class. This method is suitable for separating two classes; in this case, a value of 1 was assigned to pixels with canga, and a value of 0 was assigned to background pixels.

The training of the models took approximately 5 hours using the graphics processing unit (GPU) on an Nvidia GeForce GTX-1660Ti with 6 Gb of dedicated memory. The prediction of canga cover in a single image using the GPU took approximately 35 minutes. The model was coded in the R language (R Core Team 2016) with the RStudio interface to Keras (Chollet et al. 2015, Allaire & Chollet 2016) and a Tensor Flow backend (Abadi et al. 2016).

We applied an additional verification to observe convergences of the model prediction with the available geological mapping data in the Peixe Bravo River Valley region because the canga duricrusts are geologically associated with the rocks of the Riacho Poções Member, specifically the hematitic/iron rich metadiamictites and banded iron formations. For this purpose, the locations of some canga patches generated in model prediction to check the field areas in November 2020 and February 2021 were used. Field observations were guided using a Garmin 62S GPS model and recorded by a Nikon Coolpix P510 camera and DJI Mavic 2 UAV. Geological Service (CPRM 2021) and the Minas Gerais Economic Development Company (CODEMIG 2012). Open source QGIS software (QGIS Development Team 2009) was used to validate the delimitations.

3. Degree of direct threat to canga ecosystems

The degree of threat was estimated by superimposing the map of the canga ecosystems obtained using the U-Net model with mining concession areas in the Availability and Mining Requirement phases, available on the online platform of the Geographic Information System for Mining (SIGMINE, the acronym in Portuguese) (ANM 2021). In these phases, the mining company must present an economic use plan (PAE, the acronym in Portuguese) to the National Mining Agency (ANM, the acronym in Portuguese), the federal regulatory agency responsible for the management of mineral resources. The PAE produced by the mining company specifies, for example, the volume of mineral extraction, the economics of the enterprise and the description of all the mining and processing structures that will be implemented, thus assessing whether the mining project will be profitable (MPMG 2012). We used the geospatial data related to the polygon areas in the "Availability" and "Mining Requirement" phases obtained from ANM (2021). The overlapping areas were calculated using open source QGIS software (QGIS Development Team 2009).

Results

1. Classification and mapping of the canga ecosystems

The segmentation of cangas with the U-Net model in the 1031 images in the validation dataset had an overall accuracy of 98.5% and

Table 2. Numerical evaluation of the models and convergence details.

Model	Epoch	Batch	Sample		Overall accuracy	F1 score	Precision	Recall
			Training	Validation				
Canga cover	240	4	2061	1031	98.5%	0.8235	0.7937	0.855

Table 3. Confusion Matrix.

Confusion Matrix		Predicted label	
		Canga	No-Canga
True label	Canga	True Positive 0.74	False Negative 0.26
	No-Canga	False Positive 0.01	True Negative 0.99

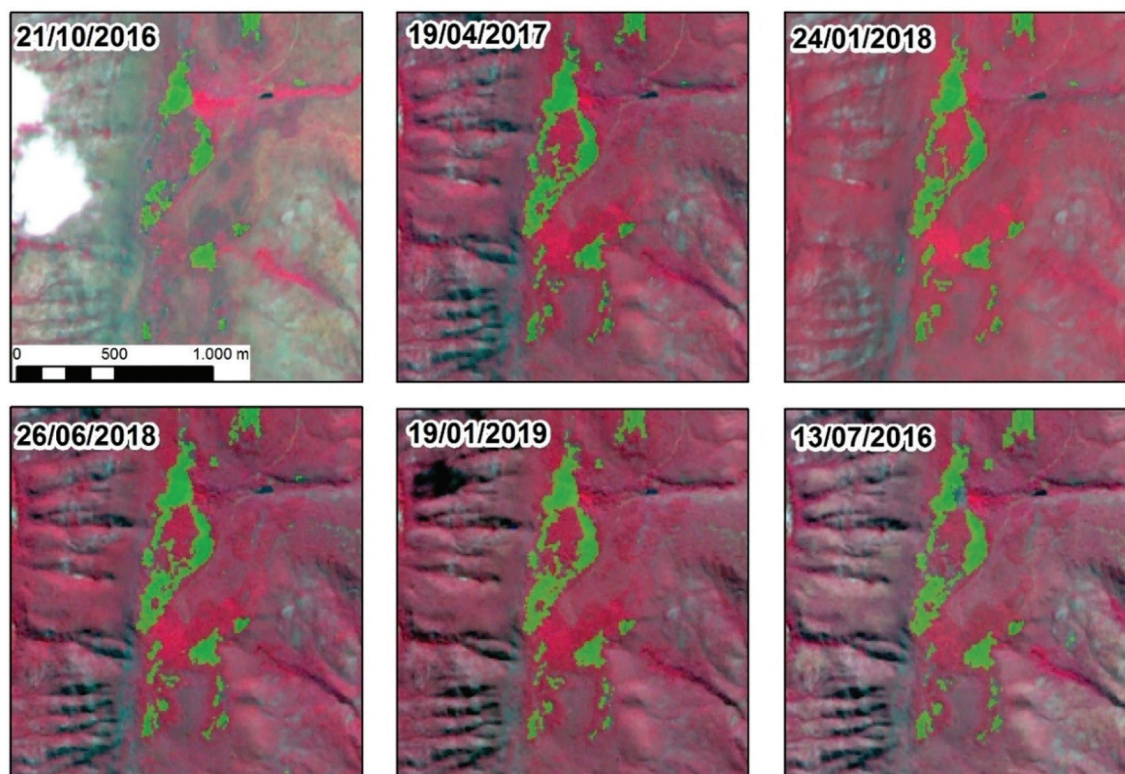Mapping canga ecosystems using U-Net deep learning

Figure 5. Details of the segmentation process for the six images observed in Sentinel-2 in July and October/2016, April/2017, January and June/2018 and January/2019 to which the model was applied. The green patches in the images represent the predicted "canga patches" on different dates.

an *F*1 score of 0.8235 (precision = 0.7937 and recall = 0.855). The time required for convergence was approximately 12 hours. The best model was obtained after 240 epochs with four images per batch (Table 2). The number of pixels correctly classified as canga as a percentage were 74% (true positive), while 26% were not detected (false negative). For background, defined as all other land covers that are not canga, the matrix indicates that 1% were detected as Canga (false positive), and 99% were classified as background (true negative) (Table 3).

The results of the canga segmentation for the Peixe Bravo River Valley, as seen in Figure 5, showed the delineation of the canga patches among the different Sentinel images. We selected the images using the sentinel metadata, which indicates the percentage of cloud cover. For training the model, we chose zero percent cloud cover. When we performed the classification, we purposely aimed to demonstrate its performance and acquired one image sensed on 10/21/2016, which showed a slightly different prediction result, likely due to a higher cloud cover. Cloud cover increased during the wet season, which occurred between September and March in this region. The surface of the land cover type of interest (a dark rocky substrate and sparse vegetation) posed another challenge because the deep learning technique is usually applied to images with features that reflect in the visible spectrum (i.e., in the RGB channels) (Wagner et al. 2019, 2020a, b). Thus, we adapted the approach for modeling canga surfaces because the infrared frequencies generated a greater contrast with the other covers (shrub and tree vegetation and water). The images were converted to the natural color composition. However, at the time of data and model preparation, removal of the blue band and insertion of the infrared range (IRG), leading to a false color composition (R8G4B2), led to a better visual result for prediction than the natural color images (Figure 5). This result

was due to the increased contrast between the target land cover (i.e., the cangas) and the rest of the surfaces (background) when using the near infrared range. In addition, removing the blue wavelengths could have reduced the noise caused by Rayleigh scattering (Jensen & Epiphanio 2011), resulting in better canga predictions.

In our set of images, the largest canga area was predicted in June 2018 (the driest period of the year), with an area of 3,330,484 m² (bottom left corner in Figure 4). In October 2016, however, the observed canga area was only 1,926,891 m² due to the presence of clouds (top left corner in Figure 5). The canga map obtained for 06/26/2018 was used in the following analyses.

The map with a 10 m spatial resolution created using U-Net deep learning allowed the identification of 762 canga patches distributed over an area of 30,000 ha. The canga ecosystems exhibited an insular distribution in the natural landscape and were concentrated in the northern part of the study area, along interfluves and on the moderate slopes of the Peixe Bravo River Valley (Figure 6). Morro Grande was another landscape compartment in which these ecosystems are concentrated; canga ecosystems were found at higher altitudes in this region (1030 m) (white arrow Figure 6), in which the largest canga patch, which was estimated to be nearly 30 ha, was observed. Cangas smaller than 1 ha represented approximately 90% of the 762 patches found in the Peixe Bravo region, and the longest linear distance between two cangas was estimated to be 43 km.

We found that most of the areas (72%) predicted to be canga by the model were associated with the lithostratigraphic unit Riacho Poções Member, represented in the geological maps at scales of 1:100,000 to 1:1,000,000. This lithostratigraphic unit contains iron-rich metadiamictite rocks. During field observations in November
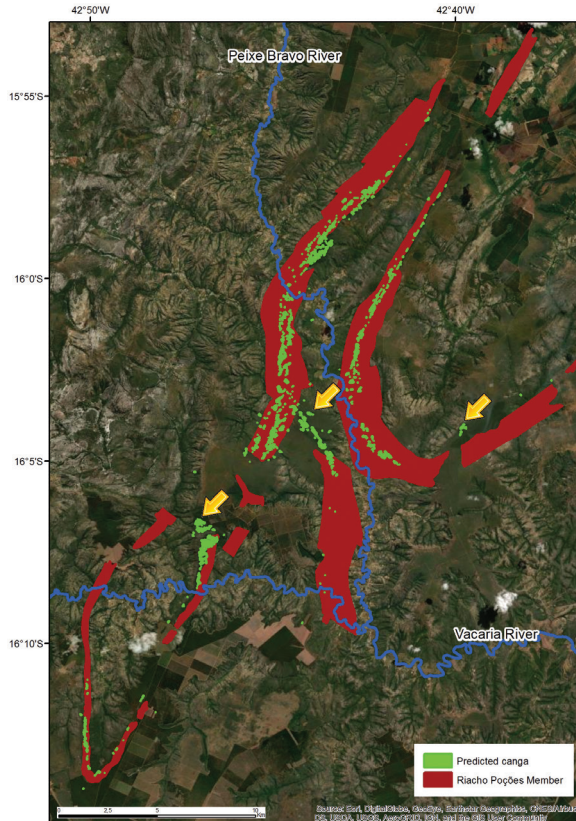
Figure 6. Predicted canga patches (green) in the Peixe Bravo River Valley and the relationship with the lithostratigraphic unit of the Riacho Poções Member/iron-rich metadiamictites (red) in geological maps (1:100,000 to 1:1,000,000). The yellow arrows indicate the main canga patches that are not yet officially identified on geological maps.

2020 and February 2021, the other canga predicted areas (28%) were verified to also be associated with the Riacho Poções Member but had not yet been identified in the officially available geological maps (Figure 6). Therefore, both the lithostratigraphic unit of the Riacho Poções Member and especially the cangas duricrusts are probably not yet fully represented in geological maps on scales of 1:100,000 to 1:1,000,000. Some canga patches predicted by the segmentation model and validated in the field presented typical cave formations associated with duricrusts (see Figure 2).

2. Degree of direct threat to canga ecosystems

Although large-scale iron ore extraction has not yet started, the opening of several access roads to hundreds of geological survey sites has caused some loss and degradation of canga ecosystems (Figure 7). We identified 26 mining concession areas in the Availability and Mining Requirement phases within the Peixe Bravo River Valley, which together cover an area of 25,064 hectares. Most of these mining concession areas were associated with the iron-rich metadiamictites of the Riacho Poções Member and, therefore, the canga duricrusts. We observed that 99.6% of the predicted canga ecosystems were included in areas with a high concentration of mining concessions (Figure 8).

Discussion

In this study, we performed the first canga ecosystem mapping in Brazil at a spatial resolution of 10 m using a U-Net convolutional network. This high-resolution mapping allowed the identification of 762 canga patches distributed in an area of 30,000 ha along the Peixe Bravo River Valley. The deep learning algorithm identified and segmented canga patches with an overall accuracy of 98.5%, demonstrating the
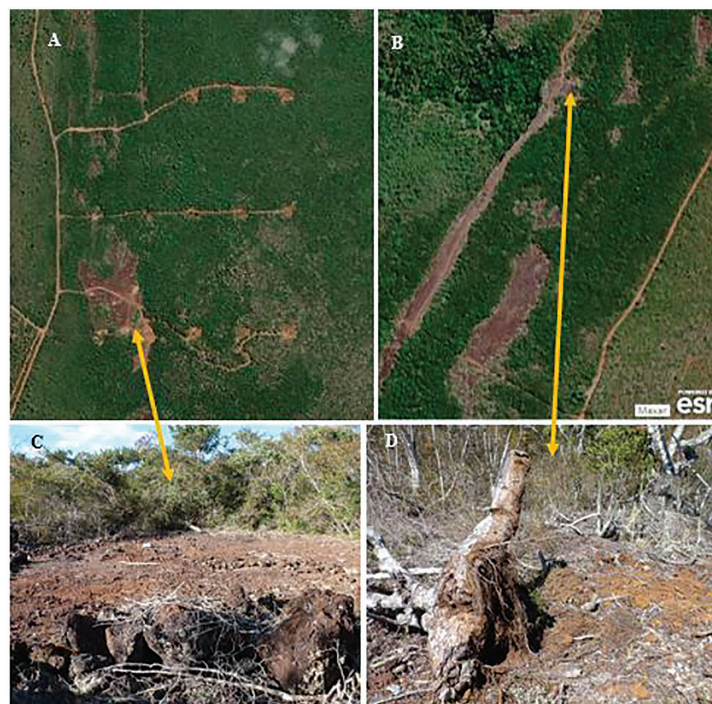

Figure 7. Environmental damage caused by geological survey sites (A and C) and access roads (B and D) resulting in degradation in canga ecosystems in the Peixe Bravo River Valley, North Minas Gerais state, southeastern Brazil. The yellow arrows indicate the relationship between the satellite images and field photos. Images A and B: Digital Geoenvironmental Atlas. Available in:https://institutopristino.org.br/atlas/municipios-de-minas-gerais/ (accessed 18 June 2022). Photos: Instituto Prístino.
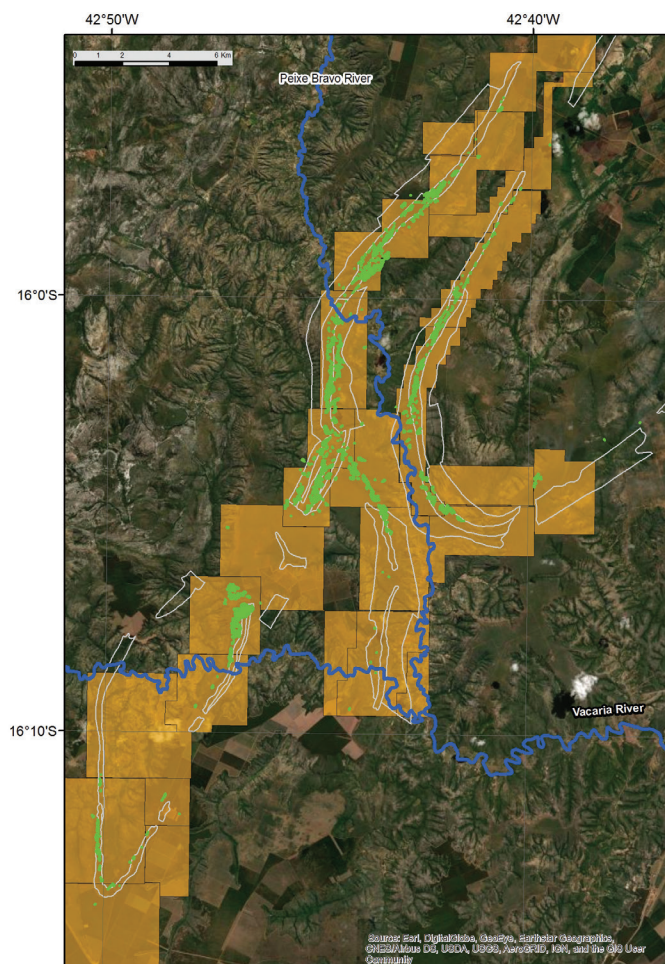
Figure 8. High concentration of mining concessions (orange polygons) in the Availability and Mining Requirement phases overlapping the predicted canga patches (green) in the Peixe Bravo River Valley, North Minas Gerais state, southeastern Brazil.

high predictive power of the map. This high level of accuracy means that for every 100 patches detected by the model, only 1.5 patches are expected to contain an error. For comparison, the accuracy of our map was superior to the overall accuracy of collection 6.0 of the Annual Mapping of Land Use and Land Coverage in Brazil (MapBiomas 2022), which reached less than 75% for Cerrado formations of the Cerrado biome, including classes 2 and 3, which correspond to grasslands and subshrub formations (including the Cerrado rupestre).

We found that obtaining images during the dry period was important for mapping rocky outcrop ecosystems located in regions that experience water stress, as was the case for the present study. During the dry period, several species partially or completely lose their aboveground biomass, while others survive despite almost complete desiccation (Proctor & Tuba 2002), which lowers the greenness of the vegetation and further exposes canga duricrusts. Acquiring images during the wet period is not an impediment; however, for long-term monitoring studies, defining a reference month for images is suggested so that the exposure conditions of the cangas are similar. This could prevent overestimation or underestimation of possible changes, such as the eventual loss or degradation of a habitat.

The mapping and monitoring of habitats and ecosystems is one of the main components of the National Biodiversity Policy (Brasil 2002),

which also recognizes that canga ecosystems are unique environments that are highly threatened by mining activities. Moreover, one of the main difficulties in implementing monitoring programs with high-resolution imagery is the high cost, which prevents the mapping of large areas (Flood et al. 2019). Thus, the challenge that our study addressed was the need for an effective but low-cost method using satellite images and free software. Previous studies generally used satellite imagery with high cost and a spatial resolution of <3 meters (Wagner et al. 2019, 2020a, b). Here, we demonstrated that for the canga ecosystem, which can be visually assessed in high-resolution images, maps used for monitoring can be created with open source software (R packages citation and keras) and with free high-resolution multispectral satellite imagery (e.g., Sentinel-2 images, which have a repeat interval of 10 days).

Using geotechnologies and artificial intelligence capable of mapping and monitoring ecosystems with restricted and naturally insular areas is essential for obtaining spatial information at the microscale (<<1 km^2). This is a common need when mapping rocky outcrop ecosystems (Cartwright 2019, Christin et al. 2019, Dang et al. 2022). The present study showed that most canga ecosystems were distributed in patches smaller than 1 ha, and nearly one-third of all predicted canga ecosystems were also associated with the Riacho Poções Member but not yet identified in the officially available geological maps. These small outcrops are essential, both because they represent exclusive habitats for endemic species (Hopper et al. 2021) and because they contribute to connectivity, serving as connection points (i.e., stepping stones) for the ecological flow between areas (Chetkiewicz et al. 2006). Thus, our results may also support conservation strategies based on studies involving spatial dynamics in plant populations and landscape ecology, including connectivity analysis (Salles et al. 2019, Ghehi et al. 2020).

In addition, Brazil has the highest plant biodiversity in the world, and Minas Gerais state has the greatest number of rare plants found in rocky outcrops (sensu lato Campos Rupestres). Because of this high conservation value and the low quality or absence of spatial occurrence data for plant species, there are enormous challenges related to monitoring the conservation status of the species in these ecosystems and conducting risk assessments for extinction (Martinelli & Mores 2013). Thus, the use of remote images with high spatial resolution and U-Net deep learning to map canga patches is a promising approach to improve our understanding of, for example, connectivity and gene flow; identify the main anthropogenic threats to conservation targets; develop appropriate guidelines and goals to prevent biodiversity losses and the degradation of ecosystem services; and determine the extent of occurrence and area of occupancy of plant populations with restricted distributions (Kiesecker et al. 2009, Pettorelli et al. 2014).

A real-world scenario in which our results could be applied is to support an evaluation of the extinction risk categories of a rare bromeliad species, *Orthophytum minimum* (Leme & O.B.C. Ribeiro), recently described in the Peixe Bravo River Valley. This rare bromeliad is endemic to canga and has a very restricted geographic distribution, being found in only one location known as Morro do Capim (Leme et al. 2020). The taxonomists who described *O. minimum* were not able to determine the extent of the canga ecosystems, and therefore, there is no information on the geographic distribution and population size of this species. Thus, *O. minimum* is considered a "data deficient" (DD) species since the available data are not sufficient for an assessment of its risk of extinction. Specifically, for the Morro do Capim location, the

present study mapped canga patches totaling less than 1 km². Thus, our study contributed directly to the application of the IUCN geographic distribution criteria (IUCN 2022) used to evaluate the threat category of a species. Another important contribution of this mapping effort is that it reduces the costs of field work associated with botanical inventories, thus making resources available to investigate more canga rather than using them to search an area of 30,000 ha. The increase in the collection effort in canga ecosystems is necessary and promising, considering that the only a floristic study published for the region (Mota et al. 2017) indicated four new species to science.

Salafsky et al. (2008) conceptualized "direct threats" as synonymous with sources of stress and proximal pressures, representing human activities that have caused, are causing, or may cause the destruction, degradation, and/or biodiversity loss. In this context, we determined there to be a high degree of direct threat to canga ecosystems in the Peixe Bravo River Valley according to the estimate that 99.6% of canga patches are included in mining concession areas (in the availability and requirement phases). This situation makes the deposits of iron ore technically and economically usable because mineral research has already been conducted and approved by the ANM (Brasil 2018). Mining entrepreneurs already have satisfied the legal conditions for initiating an environmental licensing request. In fact, there are three different mining companies that have signed protocols of intention with the State of Minas Gerais for the large-scale exploitation of iron ore over extensive natural areas. At least one mining company has already begun the application for environmental licensing in the Peixe Bravo River Valley region. This requirement is linked to a project that predicts an annual production of 27 million tons of iron ore concentrate, with the installation of open pits, tailings dams, mineral processing plants and pipelines (Minas Gerais 2021, GESTA 2022). These projects have already catalyzed socioenvironmental conflicts in a region that has not yet planned suffered major human interventions due to its rugged relief and primary land use and occupation, which is restricted to family farming distributed in small properties and traditional communities and Quilombo remnants (Carmo et al. 2011, EJatlas 2021a, Palmares Cultural Foundation 2021).

There are still no protected areas for canga ecosystems in the Peixe Bravo River Valley. Thus, our mapping could also contribute to the implementation of public policies aimed at indicating priority conservation areas (PCAs), promoting the sustainable use of resources and sharing biodiversity benefits (MMA 2021). One of the premises of the National Biodiversity Policy (Brasil 2002) is the expansion of the capacity to monitor and evaluate the impacts of natural areas with transparency, greater participation and social control. In addition, broad adherence to systematic PCA procedures is based on the adoption of ecological criteria, participatory decision-making, and the use of geotechnological tools, which are fundamental in scenarios of increasingly scarce financial resources (Margules et al. 2002, McIntosh et al. 2017). Therefore, identifying conservation targets, such as natural habitats that contain relevant biodiversity plots, provide ecosystem services and ensure the livelihood of traditional peoples and communities, is a fundamental part of the process of defining PCAs (Brasil 2005).

Acknowledgments

Associate Editor

Alexander Vibrans

Author Contributions

Eric Oliveira Pereira: Conceptualization; methodology; writing – original draft, review & editing.

Fabien H. Wagner: Methodology; writing – original draft, review & editing.

Luciana Hiromi Yoshino Kamino: Project administration; writing – original draft, review & editing.

Flávio Fonseca do Carmo: Project administration; writing – original draft, review & editing.

Conflicts of Interest

The authors declare that they have no conflicts of interest related to the publication of this manuscript.

Ethics

This study did not involve human beings and/or clinical trials that would require approval by an Institutional Committee.

Data Availability

The datasets generated during and/or analyzed during the current study are available at: https://doi.org/10.5281/zenodo.6762185

References

ABADI, M., AGARWAL, A., BARHAM, P., BREVDO, E., CHEN, Z., CITRO, C., CORRADO, G.S., DAVIS, A., DEAN, J., DEVIN, M., GHEMAWAT, S., GOODFELLOW, I., HARP, A., IRVING, G., ISARD, M., JIA, Y., JOZEFOWICZ, R., KAISER, L., KUDLUR, M., LEVENBERG, J., MANÉ, D., MONGA, R., MOORE, S., MURRAY, D., OLAH, C., SCHUSTER, M., SHLENS, J., STEINER, B., SUTSKEVER, I., TALWAR, K., TUCKER, P., VANHOUCKE, V., VASUDEVAN, V., VIÉGAS, F., VINYALS, O., WARDEN, P., WATTENBERG, M., WICKE, M., YU, Y. & ZHENG, X. 2016. TensorFlow: Large-Scale Machine Learning on Heterogeneous Systems. Software available from tensorflow.org. https://doi.org/10.48550/arXiv.1603.04467

ALLAIRE, J. & CHOLLET, F. 2016. keras: R Interface to 'Keras'. R package version 2.1.4.

ANM – AGÊNCIA NACIONAL DE MINERAÇÃO. 2020. Anuário Mineral Brasileiro: principais substâncias metálicas. ANM, Brasília. Available from: https://www.gov.br/anm/pt-br/centrais-de-conteudo/publicacoes/serie-estatisticas-e-economia-mineral/anuario-mineral/anuario-mineral-brasileiro/amb_2020_ano_base_2019_revisada2_28_09.pdf (accessed: 17 June 2022).

ANM – AGÊNCIA NATIONAL DE MINERAÇÃO. 2021. SIGMINE Sistema de Informações Geográficas da Mineração. Dados das poligonais dos processos minerários. Available from: https://dados.gov.br/dataset/sistema-de-informacoes-geograficas-da-mineracao-sigmine (accessed: 01 June 2022)

BRASIL. 2002. Decreto 4.339, 22 de agosto de 2002. Institui princípios e diretrizes para a implementação da Política Nacional da Biodiversidade. Available from: http://www.planalto.gov.br/ccivil_03/decreto/2002/d4339.htm (accessed: 17 June 2022).

BRASIL. 2005. Deliberação CONABIO n° 39, 14 de dezembro de 2005. Dispõe sobre a aprovação da metodologia para revisão das Áreas Prioritárias para a Conservação, Utilização Sustentável e Repartição de Benefícios da Biodiversidade Brasileira. Available from: http://areasprioritarias.mma.gov.br/images/arquivos/Delib_039.pdf (accessed: 17 June 2022).

BRASIL. 2018. Decreto n° 9.406, 12 de junho de 2018. Regulamenta o Decreto-Lei nº 227, 28 de fevereiro de 1967, a Lei nº 6.567, 24 de setembro de 1978, a Lei nº 7.805, 18 de julho de 1989, e a Lei nº 13.575, 26 de dezembro de 2017. Available from: http://www.planalto.gov.br/ccivil_03/_Ato2015-2018/2018/Decreto/D9406.htm (accessed: 17 June 2022).

CARDINALE, B.J., DUFFY, J.E., GONZALEZ, A., HOOPER, D.U., PERRINGS, C., VENAILS, P., NARWANI, A., MACE, G.M., TILMAN, D., WARDLE, D.A., KINZIG, A.P., DAILY, G.C., LOREAU, M., GRACE, J.B., LARIGAUDERIE, A., SRIVASTAVA, D.S. & NAEEM, SHAHID. 2012. Biodiversity loss and its impact on humanity. Nature 486:59–67. https://doi.org/10.1038/nature11148

CARMO, F.F., CARMO, F.F., SALGADO, A.A. & JACOBI, C.M. 2011. Novo sítio espeleológico em sistemas ferruginosos no Vale do Rio Peixe Bravo, Norte de Minas Gerais, Brasil. Espeleo-Tema 22:25-39. Available from: http://www.cavernas.org.br/espeleo-tema/espeleo-tema_v22_n1_025-039.pdf (accessed: 17 June 2022).

CARMO, F.F. & KAMINO, L.Y.H. (eds). 2017. O Vale do Rio Peixe Bravo: ilhas de ferro no sertão mineiro. 3i, Belo Horizonte. Available from: https://institutopristino.org.br/wp-content/uploads/2020/04/Vale-do-Rio-Peixe-Bravo_WEB-VF.pdf (accessed: 17 June 2022).

CARMO, F.F., MOTA, R.C., KAMINO, L.H.Y. & JACOBI, C.M. 2018. Checklist of vascular plant communities on ironstone ranges of south-eastern Brazil: dataset for conservation. Biodivers. Data J. 6:e27032. https://doi.org/10.3897/BDJ.6.e27032

CARMO, F.F., LANCHOTTI, A.O. & KAMINO, L.H.Y. 2020. Mining Waste Challenges: Environmental Risks of Gigatons of Mud, Dust and Sediment in Megadiverse Regions in Brazil. Sustain. 12(20), 8466. https://doi.org/10.3390/su12208466

CARTWRIGHT, J. 2019. Ecological islands: conserving biodiversity hotspots in a changing climate. Front. Ecol. Environ. 17:331–340. https://doi.org/10.1002/fee.2058

CHETKIEWICZ, C.L.B., CLAIR, C.C.S., & BOYCE, M.S. 2006. Corridors for Conservation: Integrating Pattern and Process. Annu Rev Ecol Evol Syst 37:317–342. https://doi.org/10.1146/annurev.ecolsys.37.091305.110050

CHOLLET, F., et al. 2015. Keras. Available from:https://keras.io (accessed: 17 June 2022).

CHRISTIN, S., HERVET, É. & LECOMTE, N. 2019. Applications for deep learning in ecology. Methods Ecol. Evol. 10:1632–1644. https://doi.org/10.1111/2041-210X.13256

CODEMGE – COMPANHIA DE DESENVOLVIMENTO DE MINAS GERAIS. 2018. Recursos Minerais de Minas Gerais On Line. Available from: http://recursomineralmg.codemge.com.br/wp-content/uploads/2018/10/Ferro.pdf (accessed: 17 June 2022).

CODEMIG – COMPANHIA DE DESENVOLVIMENTO ECONÔMICO DE MINAS GERAIS. 2012. Mapas geológicos do Projeto Espinhaço. Available from: http://www.portalgeologia.com.br/index.php/mapa/ (accessed: 17 June 2022).

CPRM – SERVIÇO GEOLÓGICO DO BRASIL. 2021. Sistema de Geociências do Brasil GeoSGB. Available from: https://geoportal.cprm.gov.br/geosgb/ (accessed: 17 June 2022).

DANG, K.B., NGUYEN, T.H.T., NGUYEN, H.D., TRUONG, Q.H., VU, T.P., PHAM, H.N., DUONG, T.T., GIANG, V.T., NGUYEN, D.M., BUI, T.H. & BURKHARD, B. 2022. U-shaped deep-learning models for island ecosystem type classification, a case study in Con Dao Island of Vietnam. One Ecosyst. 7: e79160. https://doi.org/10.3897/oneeco.7.e79160

EJATLAS. 2021a. Iron ore mining and mineroduct conflict, Grão Mogol, Minas Gerais, Brazil. In: Atlas of Environmental Justice. Available from: https://ejatlas.org/conflict/iron-ore-mining-and-mineroduct-grao-mogol-minas-gerais-brazil (accessed 20 January 2021).

EJATLAS. 2021b. Rio Tinto / BHP's iron mining destroys sacred Aboriginal sites, Western Australia. In: Atlas of Environmental Justice. Available from: https://ejatlas.org/conflict/rio-tintos-iron-mine-and-destruction-of-sacred-aboriginal-sites-australia (accessed 20 January 2021).

ENGLISH, V. & KEITH, D.A. 2015. Assessing risks to ecosystems within biodiversity hotspots: a case study from southwestern Australia. Austral Ecol. 40:411–422. https://doi.org/10.1111/aec.12177

ESA – EUROPEAN SPACE AGENCY. 2015. Sentinel-2. User Handbook. ESA Standard Document. Available from: https://sentinel.esa.int/documents/247904/685211/Sentinel-2_User_Handbook.pdf/8869acdf-fd84-43ec-ae8c-3e80a436a16c?t=1438278087000 (accessed 20 January 2021).

FLOOD, N., WATSON, F. & COLLETT, L. 2019. Using a U-net convolutional neural network to map woody vegetation extent from high resolution satellite imagery across Queensland, Australia. Int. J. Appl. Earth Obs. Geoinf. 82 101897-101897. https://doi.org/10.1016/j.jag.2019.101897

FONSECA, C.R., PATERNO, G.B., GUADAGNIN, D.L., VENTICINQUE, E.M., OVERBECK, G.E., GANADE, G., METZGER, J.P., KOLLMANN, J., SAUER, J., CARDOSO, M.Z., LOPES, P.F.M., OLIVEIRA, R.S., PILLAR, V.D. & WEISSER, W.W. 2021. Conservation biology: four decades of problem- and solution-based research, Perspect. Ecol. Conserv. 19:121–130. https://doi.org/10.1016/j.pecon.2021.03.003

FUNDAÇÃO CULTURAL PALMARES. 2021. Certidões Expedidas às Comunidades Remanescentes de Quilombos. Available from: http://www.palmares.gov.br/wp-content/uploads/2015/07/COMUNIDADES-CERTIFICADAS-23-11-2018-site.pdf (accessed 20 January 2021).

GESTA – GRUPOS DE PESQUISAS EM TEMÁTICAS AMBIENTAIS DA UFMG. 2022. Resistência e Luta Contra a Instalação de Projetos de Mineração de Ferro nas Microrregiões de Grão Mogol e Salinas. Available from: https://conflitosambientaismg.lcc.ufmg.br/conflito/?id=552 (accessed 20 January 2021).

GHEHI, N.K., MALEKMOHAMMADI, B. & JAFARI, H. 2020. Integrating habitat risk assessment and connectivity analysis in ranking habitat patches for conservation in protected areas. J. Nat. Conserv. 125867. https://doi.org/10.1016/j.jnc.2020.125867

GIBSON, N., YATES, C.J. & DILLON, R. 2010. Plant communities of the ironstone ranges of South Western Australia: hotspots for plant diversity and mineral deposits. Biodivers Conserv 19:3951–3962. https://doi.org/10.1007/s10531-010-9939-1

GOOGLE. 2021. Google Earth Pro. Google LLC.

HARDNER, J., GULLISON, R.E., ANSTEE, S., MEYER. M. 2015. Boas práticas para a avaliação de impacto e o planejamento da gestão incluindo a biodiversidade. Preparado para o Grupo de Trabalho sobre Biodiversidade para Instituições Financeiras Multilaterais. Available from: https://publications.iadb.org/en/good-practices-biodiversity-inclusive-impact-assessment-and-management-planning (accessed 10 December 2022).

HOPPER, S.D., LAMBERS, H., SILVEIRA, F.A. & FIEDLER, P.L. 2021. OCBIL theory examined: reassessing evolution, ecology and conservation in the world's ancient, climatically buffered and infertile landscapes. Biol. J. Linn. Soc. 133(2):266–96. https://doi.org/10.1093/biolinnean/blaa213

IBGE. INSTITUTO BRASILEIRO DE GEOGRAFIA E ESTATÍSTICA. 2012. Manual técnico da vegetação brasileira: sistema fitogeográfico, inventário das formações florestais e campestres, técnicas e manejo de coleções botânicas, procedimentos para mapeamentos. Coordenação de Recursos Naturais e Estudos Ambientais. - 2. ed., Rio de Janeiro, 276 p.

IUCN STANDARDS AND PETITIONS COMMITTEE. 2022. Guidelines for Using the IUCN Red List Categories and Criteria. Version 15. Prepared by the Standards and Petitions Committee. Available from: https://www.iucnredlist.org/documents/RedListGuidelines.pdf. (accessed 17 June 2022).

JACOBI, C.M., CARMO, F.F. & CAMPOS, I.C. 2011. Soaring Extinction Threats to Endemic Plants in Brazilian Metal-Rich Regions. AMBIO 40:540–543. https://doi.org/10.1007/s13280-011-0151-7

JENSEN, J.R. & EPIPHANIO, J.C.N. 2011. Sensoriamento remoto do ambiente: uma perspectiva em recursos terrestres. Editora Parêntese, São José dos Campos.

KIESECKER, J.M., COPELAND, H., POCEWICZ, A., NIBBELINK, N., MCKENNEY, B., DAHLKE, J., HOLLORAN, M. & STROUD, D. 2009. A framework for implementing biodiversity offsets: selecting sites and determining scale. Bioscience 59: 77–84. https://doi.org/10.1525/bio.2009.59.1.11

KIM, S. 2020. Deep learning with R. (Orgs.), Chollet, F. & Allaire, J.J. Shelter Island, NY: Manning. Biometrics, 76 (1): 361–362. https://doi.org/10.1111/biom.13224

KRIZHEVSKY, A., SUTSKEVER, I. & HINTON, G.E. 2017. ImageNet Classification with Deep Convolutional Neural Networks. Communications of the ACM 60 (6):84–90. https://doi.org/10.1145/3065386

LAMBA, A., CASSEY, P., SEGARAN, R.R. & KOH, L.P. 2019. Deep learning for environmental conservation. Curr. Biol. 29(19):PR977-R982. https://doi.org/10.1016/j.cub.2019.08.016

LECUN, Y., BENGIO, Y. & HINTON, G. 2015. Deep learning. Nature 521,436–444. https://doi.org/10.1038/nature14539

LECUN, Y., BOTTOU, L., BENGIO, Y. & HAFFNER, P., 1998. Gradient-based learning applied to document recognition. Proc. IEEE 86, 2278–2324. https://doi.org/10.1109/5.726791

LEME, E.M., RIBEIRO, O.B., SOUZA, F.V.D., DE SOUZA, E.H., KOLLMANN, L.J. & FONTANA, A.P. 2020. Miscellaneous new species in the "Cryptanthoid complex" (Bromeliaceae: Bromelioideae) from Eastern Brazil. Phytotaxa 430(3):157–202. https://doi.org/10.11646/phytotaxa.430.3.2

MAPBIOMAS. 2022. Coleção 6.0 da Série Anual de Mapas de Cobertura e Uso de Solo do Brasil. Available from: https://mapbiomas.org/accuracy-statistics (accessed 20 April 2022)

MARGULES, C.R., PRESSEY, R.L. & WILLIANS, P.H. 2002. Representing biodiversity: data and procedures for identifying priority areas for conservation. J. Biosci. 27: 09–326 https://doi.org/10.1007/BF02704962

MARTINELLI, G. & MORAES, M.A. (Ed) 2013. Livro Vermelho da Flora do Brasil. Instituto de Pesquisa Jardim Botânico do Rio de Janeiro, Rio de Janeiro.

MCINTOSH, E.J., PRESSEY, R.L., LLOYD, S., SMITH, R.J. & GRENYER, R. 2017. The Impact of Systematic Conservation Planning. Annu. Rev. Environ. Resour 42:677–697. https://doi.org/10.1146/annurev-environ-102016-060902

MELFI, A.J., MISI, A., CAMPOS, D.A.C. & CORDANI, U.G. (ed) 2016. Recursos Minerais no Brasil: problemas e desafios. Academia Brasileira de Ciências, Rio de Janeiro.

MINAS GERAIS. 2021. Mineração no Norte de Minas gera polêmica. Available from: https://www.almg.gov.br/acompanhe/noticias/arquivos/2021/08/25_mineracao_no_norte_de_minas_gera_polemica (accessed 17 June 2022).

MMA – MINISTÉRIO DO MEIO AMBIENTE. 2000. A Convenção sobre Diversidade Biológica – CDB. Série Biodiversidade no. 2. Brasília – DF. Available from: https://www.gov.br/mma/pt-br/textoconvenoportugus.pdf (accessed 17 November 2022).

MMA – MINISTÉRIO DO MEIO AMBIENTE. 2021. Áreas Prioritárias para a Conservação da Biodiversidade Brasileira. Available from: http://areasprioritarias.mma.gov.br/ (accessed 17 June 2022).

MPMG – MINISTÉRIO PÚBLICO DE MINAS GERAIS. 2012. Guia Técnico para atuação do Ministério Público no licenciamento ambiental de atividades de mineração. MPMG, Belo Horizonte.

MOTA, R.C., KAMINO, L.H.Y. & CARMO, F.F. 2017. Levantamento florístico preliminar das plantas vasculares do Geossistema Ferruginoso do Vale do Rio Peixe Bravo. In: O Vale do Rio Peixe Bravo: ilhas de ferro no sertão mineiro (F.F. Carmo & L.H.Y. Kamino, eds). 3i, Belo Horizonte. Available from: https://institutopristino.org.br/publicacoes/ (accessed 17 June 2022).

PETTORELLI, N., SAFI, K. & TURNER, W. 2014. Satellite remote sensing, biodiversity research and conservation of the future. Phil. Trans. R. Soc. B 369:20130190. http://dx.doi.org/10.1098/rstb.2013.0190

PROCTOR, M.C. & TUBA, Z. 2002. Poikilohydry and homoihydry: antithesis or spectrum of possibilities? New Phytol. 156:327–349. https://doi.org/10.1046/j.1469-8137.2002.00526.x

QGIS DEVELOPMENT TEAM. 2009. QGIS Geographic Information System. Open Source Geospatial Foundation.

R CORE TEAM. 2016. R: A Language and Environment for Statistical Computing. R Foundation for Statistical Computing, Vienna, Austria.

REBOITA, M.S., RODRIGUES, M., SILVA, L. F. & ALVES, M.A. 2015. Aspectos climáticos do estado de Minas Gerais. Rev. Bras. Climatol. 17:206–226. http://dx.doi.org/10.5380/abclima.v17i0.41493

RONNEBERGER, O., FISCHER, P. & BROX, T. 2015. U-net: Convolutional networks for biomedical image segmentation. In Medical Image Computing and Computer-Assisted Intervention – MICCAI 2015. (N. Navab, J. Hornegger, W. Wells & A. Frangi, eds) Lect. Notes Comput. Sci. vol 9351. Springer, Cham. https://doi.org/10.1007/978-3-319-24574-4_28

SALAFSKY, N., SALZER, D., STATTERSFIELD, A.J., HILTON-TAYLOR, C., NEUGARTEN, R., BUTCHART, S.H.M., COLLEN, B., COX, N., MASTER, L.L., O'CONNOR, S. & WILKIE, D. 2008. A standard lexicon for biodiversity conservation: unified classifications of threats and actions. Conserv. Biol. 22:897–911. https://doi.org/10.1111/j.1523-1739.2008.00937.x

SALLES, D.M., CARMO, F.F. & JACOBI, C.M. 2019. Habitat Loss Challenges the Conservation of Endemic Plants in Mining-Targeted Brazilian Mountains. Environ Conserv 46:140–146. https://doi: 10.1017/S0376892918000401

SÁNCHEZ, L.E., ALGER, K., ALONSO, L., BARBOSA, F.A.R., BRITO, M.C.W., LAUREANO, F.V., MAY, P., ROESER, H. & KAKABADSE, Y. 2018. Impacts of the Fundão Dam failure. A pathway to sustainable and resilient mitigation. Rio Doce Panel Thematic Report No. 1. Gland. IUCN, Switzerland. https://doi.org/10.2305/IUCN.CH.2018.18.en

SENTINEL DATA HUB. 2020. Available from: https://scihub.copernicus.eu/dhus/#/home (accessed 18 March 2020)

SONTER, L.J., BARRETT, D.J., SOARES-FILHO, B.S. & MORAN, C.J. 2014. Global demand for steel drives extensive land-use change in Brazil's Iron Quadrangle. Glob. Environ. Change 26:63–72. https://doi.org/10.1016/j.gloenvcha.2014.03.014

SOUZA, C.M. JR., SHIMBO J.Z., ROSA, M.R., PARENTE, L.L., ALENCAR, A.A., RUDORFF, B.F.T., HASENACK, H., MATSUMOTO, M., FERREIRA, L.G., SOUZA-FILHO, P.W.M., OLIVEIRA, S.W., ROCHA, W.F., FONSECA, A.V., MARQUES, C.B., DINIZ, C.G., COSTA, D., MONTEIRO, D., ROSA, E.R., VÉLEZ-MARTIN, E., WEBER, E.J., LENTI, F.E.B., PATERNOST, F.F., PAREYN, F.G.C., SIQUEIRA, J.V., VIERA, J.L., NETO, L.C.F., SARAIVA, M.M., SALES, M.H., SALGADO, M.P.G., VASCONCELOS, R., GALANO, S., MESQUITA, V.V. & AZEVEDO, T. 2020. Reconstructing Three Decades of Land Use and Land Cover Changes in Brazilian Biomes with Landsat Archive and Earth Engine. Remote Sens. 12(17):2735. https://doi.org/10.3390/rs12172735

TIBBETT, M. 2015. Mining in ecologically sensitive landscapes: concepts and challenges. In Mining in Ecologically Sensitive Landscapes (M. Tibbett, ed). CSIRO Publishing, Leiden.

UNEP – UNITED NATIONS ENVIRONMENT PROGRAMME (Ed.). 2019. Global Environment Outlook – GEO-6: Healthy Planet, Healthy People. Cambridge University Press, Cambridge. doi:10.1017/9781108627146

Mapping canga ecosystems using U-Net deep learning

WAGNER, F.H., SANCHEZ, A., TARABALKA, Y., LOTTE, R.G., FERREIRA, M.P., AIDAR, M.P.M., GLOOR, E., PHILLIPS, O.L. & ARAGÃO, L.E.O.C. 2019. Using the U-net convolutional network to map forest types and disturbance in the Atlantic rainforest with very high resolution images. Remote. Sens. Ecol. 5:360–375 https://doi.org/10.1002/rse2.111

WAGNER, F.H., SANCHEZ, A., AIDAR, M.P., ROCHELLE, A.L., TARABALKA, Y., FONSECA, M.G., PHILLIPS, O.L., GLOOR, E. & ARAGÃO, L.E. 2020a. Mapping Atlantic rainforest degradation and regeneration history with indicator species using convolutional network. PLoS ONE 15(2):e0229448. https://doi.org/10.1371/journal. pone.0229448

WAGNER, F.H., DALAGNOL, R., TARABALKA, Y., SEGANTINE, T.Y.F., THOMÉ, R. & HIRYE, M.C.M. 2020b. U-Net-Id, an Instance Segmentation Model for Building Extraction from Satellite Images – Case Study in the Joanópolis City, Brazil. Remote Sens. 12:1544. https://doi.org/10.3390/rs12101544